Modeling of Eruptive Episodes on X-ray Binary Systems

Author: María del Mar Carretero Castrillo
*Facultat de Física, Universitat de Barcelona, Diagonal 645, 08028 Barcelona, Spain.**

Advisor: Josep Maria Paredes Poy

Abstract: We study the X-ray binary system Cygnus X-3 radio outburst applying the van der Laan model, which considers an adiabatically expanding cloud of relativistic electrons. We fit the time evolution of the synchrotron radiation, the outburst peak flux density and time delay to the observational data of its radio outburst in 1972 September. The model reproduces the general trend of the data although some discrepancies, which are found, especially, in the low frequency range.

I. INTRODUCTION

The analogy between quasars and microquasars lead to the discovery of superluminal sources in our own galaxy, where it is possible to follow the motions of the two-side ejecta. Due to the relative proximity and shorter time scales, in microquasars it is possible to firmly establish the relativistic motion of the sources of radiation and to better study the physics of accretion flows and jet formation [6].

Microquasars are binary systems formed by a star and a compact object, which is a black hole or a neutron star, accreting matter of the companion star and creating an accretion disk, whose process involves X-ray emision [8]. These systems display collimated jets, which seem to be associated with the accreting evolution, nevertheless its emission is in the infrared and radio wavelengths.

According to the spectral type of the companion star, the X-ray binary system is classified as follow [8]:

- Low mass X-ray binaries (LMXB): the donor star is of a spectral type later than B and mass transfer takes place through Roche lobe overflow.
- High mass X-ray binaries (HMXB): the companion star is either O or B spectral type. Mass transfer takes place via decretion disc for Be star, wind accretion or Roche lobe overflow.

Collimated jets appear to be associated with the presence of an accretion disk around the compact object [7]. The multiwavelengths observations of microquasars reveal that the disapperance of the inner accretion disk with the ejection of relativistic clouds of plasma are correlated. It is believed that a portion of the rotation energy of the compact object could be use to boost the collimated outburst of magnetized plasma at relativistic speeds [6]. The interaction between the beam, the radiation and wind of the companion star or with the interstellar medium results in TeV-GeV emissions from this sources. In this way, jets extract a large fraction of the total accretion energy available [8].

The relativistic plasma cloud is observed at infrared and later at radio bands. The delay between both maximums is estimated by the van der Laan model (1966) [12] for a spherically symmetric expanding clouds in relativistic AGN jets [6].

This non-thermal emission from jets implies the presence of highly energetic electrons which may also emit in the gamma wavelenghths through inverse Compton, which is the case of Cygnus X-3, that has been confirmed as a high-energy source by AGILE and Fermi-LAT [9].

II. CYGNUS X-3

This microquasar was one of the first sources discovered in the beginnings of the radio astronomy and has motivated to a large extent the development of high energy astronomy [11]. It is one of the most attractive microquasars, with frequent flaring activity of its relativistic jets [2].

Cygnus X-3 is a high-mass X-ray binary system with a brief orbital period of 4.8 hours. We can find it in the galactic plane at a distance of ~ 7 kpc. The companion star is known to be a Wolf-Rayet, whereas the nature of the compact object remains unknown due to the interstellar absorption, which leaves the visible band undetectable [5], [11]. It is believed to be either a neutron star in an unusual state of accretion or a $10-20M_{\odot}$ black hole [1].

After its discovery in 1966, Cyg X-3 has been deeply observed over a wide wavelength range. Its variable emission extending from radio frequencies up to a few hundred of kiloeclectron volts (keV), is induced by the interaction between the stellar companion, the accretion flow shaping the disk, and the relativistic jets.

In the radio range, the binary system had several violent outbursts with flux density increments of almost 3 orders of magnitud above its usual level of $\sim 0,1Jy$ [5], which are associated with the collimated jets and reveal their variable activity. [3]. The specified makes it one of the brightest galactic transient radio sources.

*Electronic address: m.carretero.castrillo@gmail.com

The X-ray spectrum fluctuates between hard and soft states, similar to other X-ray binaries, and it is heavily absorbed at low energies by the intervening dense stellar wind. The accretion process is related with these wavelengths [2].

AGILE and Fermi Large Area Telescope (Fermi/LAT) have reported high energy gamma rays detections, denoting a clear correlation of special radio/X-ray activity, preceding strong radio flares [2], [10]. In this way, Cygnus X-3 is the first binary hosting and accreting object and relativistic jets to be detected in γ-rays. [2]

Complex as it may be, the theoretical modelling of galactic microquasars such as Cygnus X-3 require particle acceleration and non-thermal photon production up to GeV energies as crucial ingredients.

III. THE VAN DER LAAN MODEL

The van der Laan model (1966) [12] emerges as an explanation for the variability of extragalactic radio sources. Based on an initially optically thick radio source which transforms into an optically thin as it expands, the model considers a uniform and spherical cloud of radius r, at expanding rate $\dot{r}$, constituted of a flux of relativistic electrons with an isotropic velocity distribution. Thus, the energy distribution can be expressed as $N(E)dE = K(t)E^{-p}dE$, with $E_1(t) \leq E \leq E_2(t)$, where N is the number density of the electrons, $K(t)$ a time-depending constant and p the energy spectral index.

Synchrotron radiation is generated by acceleration of particles in the presence of a magnetic field, whose magnetic flux is conserved as

$$B = B_0 \left(\frac{r}{r_0}\right)^{-2}, \tag{1}$$

where r_0 is the initial radio of the source. The relativistic gas cools adiabatically,

$$E = E_0 \left(\frac{r}{r_0}\right)^{-1}, \tag{2}$$

and the angular diameter changes as

$$\theta = \theta_0 \left(\frac{r}{r_0}\right). \tag{3}$$

Furthermore, the model contemplates a constant number of the plasma particles, which imposes

$$\frac{d}{dt}\left\{r^2 K_0(r) \int_{E_1(t)}^{E_2(t)} E^{-\gamma} dE\right\} = 0. \tag{4}$$

Note that the subindex 0 is referred to the value of the parameters at the instant t_0.

For synchrotron radiation, the dependence on frequency of the volume emissivity is $p(\nu) \propto \nu^{-(p-1)/2}$ whereas the dependence of the absorption coefficient $\mu(\nu) \propto \nu^{-(p+4)/2}$. As the density flux is given by

$$\begin{aligned} S(\nu) &\propto \frac{p(\nu)}{\mu(\nu)}\left[1 - e^{-\tau(\nu)}\right] \\ &\propto \nu^{5/2}\left[1 - e^{-\tau(\nu)}\right], \end{aligned} \tag{5}$$

where τ_ν is the optical depth, expressed by $\tau_\nu \propto \nu^{-\frac{p+4}{2}}$, we can find for the optically thick region ($\nu << 1$) that $S(\nu) \propto \nu^{5/2}$, and for the optically thin ($\nu >> 1$), $S(\nu) \propto \nu^{-\frac{p-1}{2}}$.

Our aim is to find the temporal evolution of the flux density. In relation to this, the model provides the variations with the relative radius of the source $\rho = \frac{r}{r_0}$ with the maximum flux density S_m and the frequency ν_m at which it occurs

$$S_m(\rho) = S_{m0}\, \rho^{-(7p+3)/p+4}, \tag{6}$$

$$\nu_m(\rho) = \nu_{m0}\, \rho^{-(4p+6)/p+4}. \tag{7}$$

From where we can construe the qualitative form of the spectrum: in the plane $\log S(\nu) - \log \nu$, as the cloud expands, the spectral curve will move down and towards the left, but maintaining its shape. At lower frequencies, the peak will be reached later and have a smaller value, as shown in figure 1.

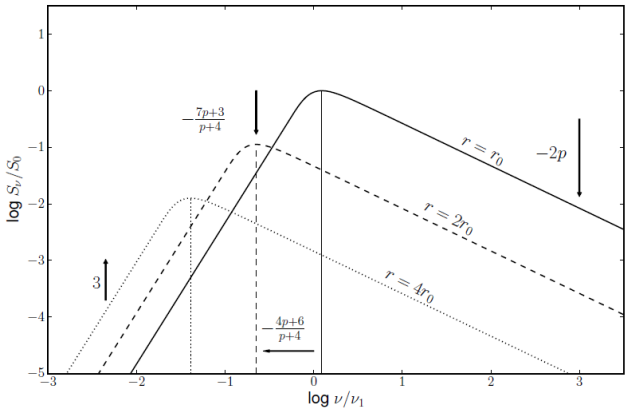

FIG. 1: Evolution of the flux density in function of the frequency of an electron cloud expanding uniformly.

Using relations (5), (6) and (7), the van der Laan model obtains the flux density at a given frequency and radius relative to their values at the spectral maximum when $\rho = 1$. Then

$$S(\nu,\rho) = S_{m0}\left(\frac{\nu}{\nu_{m0}}\right)^{\frac{5}{2}} \rho^3 \frac{1 - \exp\left\{-\tau_m \left(\frac{\nu}{\nu_{m0}}\right)^{-\frac{p+4}{2}} \rho^{-(2p+3)}\right\}}{1 - \exp(-\tau_m)}, \tag{8}$$

wherein τ_m is the optical depth corresponding at which the flux density is maximum, namely, the solution of $dS/d\nu = 0$, which gives

$$e^{\tau_m} - \left(\frac{p+4}{5}\right)\tau_m - 1 = 0. \tag{9}$$

The form of the equation (8) in function of the relative radius is illustrated in figure 2.

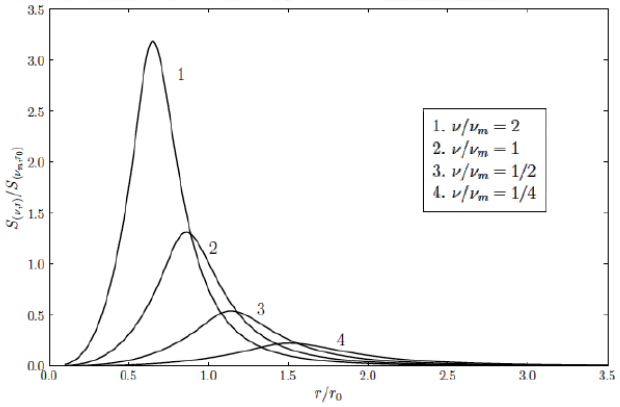

FIG. 2: Radial dependence of flux density for different frequencies. The values of the curves are shown in the legend.

In order to obtain the flux density as a function of frequency and time, the model assumes a constant expansion velocity, in this way, the radius varies as $r = r_0 + vt$. Consequently, the temporal evolution of the relative radius is

$$\rho(t) = \frac{r}{r_0} = 1 + \frac{vt}{r_0} = 1 + \frac{t'}{t_0}, \tag{10}$$

where v is the expanding velocity of the source and t' is the time measured from the instant where S_{m0} and ν_{m0} are specified.

IV. RESULTS

Here we analyze the giant radio outburst in 1972 September of Cygnus X-3, assuming synchrotron radiation the responsible of the emission process. These events are amongst the best-known examples of observed expanding synchrotron-emitting sources. The analysis of these data has focused mainly on the temporal behaviour of the radio emission.

We apply the model to the observational data obtained from [4], getting the parameters which fit curves the best. These parameters are presented in table I. The value found for the energy spectral index is $p = 1.76$.

Discrepancies from the model are discussed in the last section.

	$S_{m0}(Jy)$	$\nu_{m0}(GHz)$	p
Lower frequencies	137	1290	1.76
Higher frequencies	92	10000	1.76

TABLE I: Parameters obtained in the fit. Low frequencies refers to 0.408GHz, 1.415GHz and 2.695GHz, the optically thick region; while high frequencies to 6.630GHz and 8.085GHz, the optically thin one.

A. Radio light-curves

To obtain the temporal evolution of the flux density at a given frequency we use equation (8) taking into account the linear dependence of the relatives radius with time given by equation (10). The best fit to the curves is shown in figure 3. The frequencies plotted are 0.408GHz, 1.415GHz, 2.695GHz, 6.630GHz and 8.085GHz.

Observations at a given frequency evidence a prompt increase of flux at first, reach the maximum at S_m and a more smooth decrease. The model prediction is also checked at lower frequencies, the peak is reached later and have a smaller value. These results are presented in table II.

$\nu(GHz)$	$t_m(UTdate)$	$S_m(Jy)$
0.408	7.5	1.82
1.415	4.3	7.82
2.695	3.3	16.66
6.630	3.3	26.58
8.085	3.2	18.01

TABLE II: Values of the density flux S_m, the time at which it is reached t_m and the frequency.

B. Outburst peak flux density

The maximum flux densities for each frequency are presented in figure 4. For the observational data of the low frequency branch we obtain $S(\nu) \propto \nu^{1.15}$, whereas for the high frequency branch $S(\nu) \propto \nu^{-0.38}$.

As in the optically thin region $S(\nu) \propto \nu^{-\frac{p-1}{2}}$, we can find the energy spectral index as

$$-\frac{p-1}{2} = -0.38 \longrightarrow p = 1.76.$$

If we consider a frequency which is initially optically thick, the flux density will peak near the time at which the expansion of the jet produces the transition to the optically thin regime, fact that can be observed in the aforementioned graphic. This change varies for different jets. Obviously, the first jet cross sections to become optically thin are those ejected first [4].

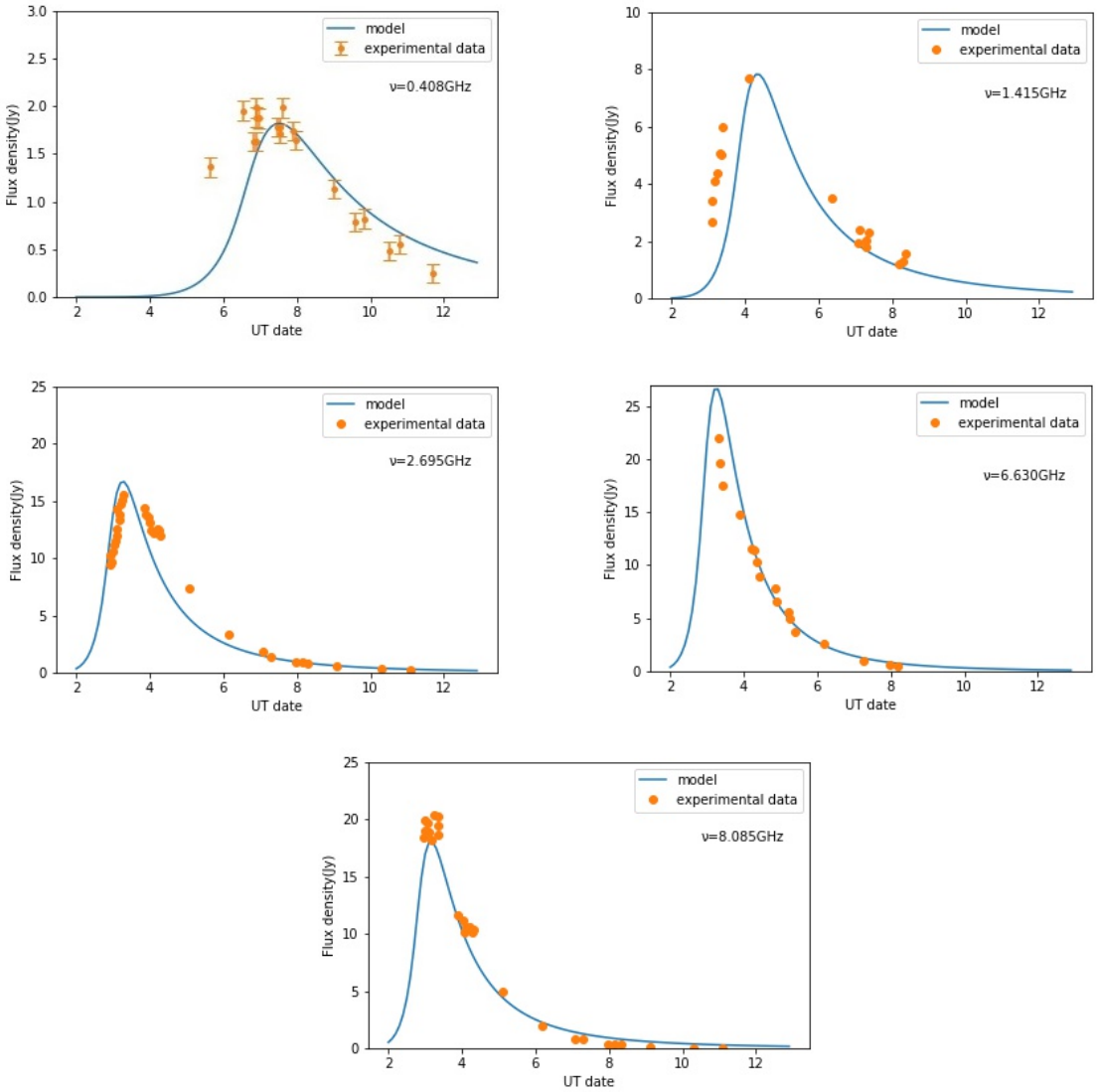

FIG. 3: Radio light-curves computed from the van der Laan model corresponding to the first strong radio outburst of Cyg X-3 in 1972 September. The error bars not shown are smaller than the symbol size.

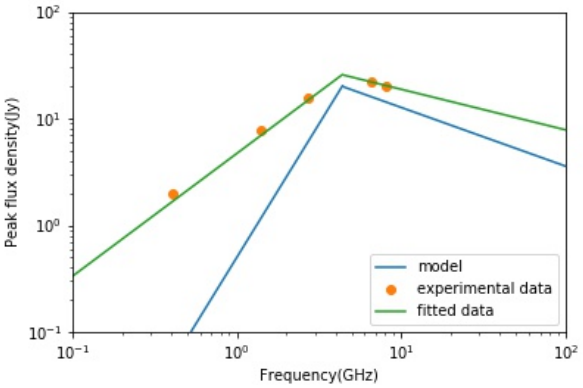

FIG. 4: Outburst peak flux density as function of frequency with the points for the same five frequencies as in figure 3. The error bars not shown are smaller than the symbol size.

C. Outburst peak time delay

The van der Laan model also provides a relation between the frequency at which the maximum flux density is reached and the time

$$\nu_m \propto t^{-\frac{4p+6}{p+4}} \rightarrow t \propto \nu_m^{-\frac{p+4}{4p+6}}. \tag{11}$$

Taking into account the exposed, the energy spectral index is $p = 1.76$, so that $t \propto \nu_m^{-0.44}$.

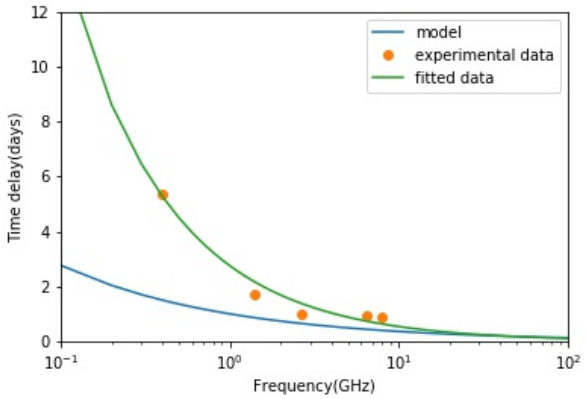

FIG. 5: Outburst peak time delay. Observed points are also included for the same five frequencies. The error bars not shown are smaller than the symbol size.

Another estimation of the model is provided in figure 5, where the peak time delay is larger for lower frequencies.

V. DISCUSSION AND CONCLUSIONS

In this paper we studied the radio outbursts of the microquasar Cygnus X-3 applying the van der Laan model. Radio light-curves, outburst peak flux density and time delay have been obtained, getting the best-fitting parameters to the observational data.

The energy spectral index obtained is $p = 1.76$, while the one from Martí et al. (2006) is $p = 2.1$, which implies a relative error of 16%. This difference is not a surprise and was expected somehow because we have used the basic van der Laan model.

As can be observed in all the graphics displayed, the basic model of van der Laan reproduce roughly the observed data, nevertheless it is less accurate for the lower frequencies. This physical reality could be explained by the free-free absorption process, which dominates in the optically thick zone, and that have not been taken into account by the van der Laan model.
Other detected discrepancies suggest that there are different features in this kind of systems that have not been considered. On the one hand, the geometry of the source is assumed spherical, while observations show a jet-like geometry. On the other hand, it has been established that the number of particles conforming the cloud remains constant, condition given by the equation (4), excluding the possibility of continuous injection of relativistic electrons and the energy losses of this particles by different processes. Additionally, other details as a constant expansion rate or a uniform cloud, could not be fulfilled so deviations from the model are expected.

The results of the spectra analysis provide a useful test of models proposed to explain the temporal variations of the flux density of Cygnus X-3 during an outburst.

Acknowledgments

I would like to thank my advisor, Dr. Josep Maria Paredes Poy, for his guidance and support, further his positive vision and comments about my work. I would also like to express my gratitud to Javier de Cruz Pérez, for his counsel and help throughout my career. Finally, render thanks to all the family and friends, for their unconditional support.

[1] Blancha O., de Oña Wilhelmib E., Galindoc D., et al. 2017 arXiv:1709.01725
[2] Corbel S., Dubus G., Tomsick J. A., et al. 2012. Mon. Not. R. Astron. Soc. 421, 2947–2955
[3] Gregory, P. C., Seaquist E. R., 1974. *The Astrophysical Journal.* Vol. 194. 715-723.
[4] Martí J., Paredes J. M., Estalella R., 1992. *Astron. Astrophys. 258, 309-315.*
[5] Martí J., Pérez-Ramírez D., Luque-Escamilla P., et al. 2006. *A&A* 451, 1037–1040
[6] Mirabel I.F., 2002 arXiv:astro-ph/0211085v1
[7] Mirabel, I. F., Rodríguez, L. F., 1999. *Annu. Rev. Astron. Astrophys.* 37:409–43
[8] Paredes J.M, 2011. *Mem. S.A.It.* Vol. 82, 174
[9] Paredes, J.M., Bordas, P., 2019 arXiv190209898P
[10] Tavani M., Bulgarelli A., Piano G., et al. 2009. *Nature.* Vol. 462, Issue 7273, 620-623
[11] The Fermi LAT Collaboration. 2009. *Science*, Vol. 326 (5959), 1512-1516
[12] van der Laan H.,1966, *Nature*, 211, 1131-1133